Improved Experimental Limit on the Electric Dipole Moment of the Neutron

C. A. Baker,[1] D. D. Doyle,[2] P. Geltenbort,[3] K. Green,[1,2] M. G. D. van der Grinten,[1,2] P. G. Harris,[2] P. Iaydjiev,[1,*] S. N. Ivanov,[1,†] D. J. R. May,[2] J. M. Pendlebury,[2] J. D. Richardson,[2] D. Shiers,[2] and K. F. Smith[2]

[1]*Rutherford Appleton Laboratory, Chilton, Didcot, Oxon OX11 0QX, United Kingdom*

[2]*Department of Physics and Astronomy, University of Sussex, Falmer, Brighton BN1 9QH, United Kingdom*

[3]*Institut Laue-Langevin, BP 156, F-38042 Grenoble Cedex 9, France*

(Received 9 February 2006; revised manuscript received 29 March 2006; published 27 September 2006)

An experimental search for an electric dipole moment (EDM) of the neutron has been carried out at the Institut Laue-Langevin, Grenoble. Spurious signals from magnetic-field fluctuations were reduced to insignificance by the use of a cohabiting atomic-mercury magnetometer. Systematic uncertainties, including geometric-phase-induced false EDMs, have been carefully studied. The results may be interpreted as an upper limit on the neutron EDM of $|d_n| < 2.9 \times 10^{-26} e$ cm (90% C.L.).

DOI: 10.1103/PhysRevLett.97.131801 PACS numbers: 13.40.Em, 07.55.Ge, 11.30.Er, 14.20.Dh

Measurements of particle electric dipole moments (EDMs) [1–3] provide some of the tightest constraints on extensions to the standard model, such as supersymmetry, that attempt to explain the mechanisms underlying *CP* violation [4–11]. This neutron-EDM experiment has been discussed in earlier publications [1,12]. The final result presented in this Letter incorporates a comprehensive analysis of systematic errors, some of which were undiscovered at the time of the earlier measurements.

The measurement was made with ultracold neutrons (UCNs) stored in a trap (Fig. 1) permeated by uniform **E** and **B** fields. The neutron spin polarization precesses about the field direction at the Larmor frequency ν:

$$h\nu = |2\mu_n B \pm 2d_n E|, \tag{1}$$

where the $+$ $(-)$ sign corresponds to parallel (antiparallel) fields. Thus, the experiment aimed to measure any shift in ν as an applied **E** field alternated between being parallel and then antiparallel to **B**.

The UCNs were prepared in a spin-polarized state by transmission through a thin, magnetized iron foil and entered a cylindrical 21-liter trap within a 1 μT uniform vertical magnetic field $\mathbf{B}_0$.

Approximately 20 s were needed to fill the trap with neutrons, after which the entrance door was closed pneumatically. The electric field, of approximately 10 kV/cm, was generated by applying high voltage (HV) to the electrode that constituted the roof of the trap, while grounding the floor electrode. The electrodes were made of diamond-like-carbon coated Al, and the side wall was SiO_2.

The transition frequency ν of the neutrons was measured using the Ramsey separated-oscillatory-field magnetic resonance method. During the storage period, the neutrons interacted coherently with two 2 s intervals of oscillating magnetic field having a chosen frequency close to the Larmor frequency. The two intervals were separated by a period $T = 130$ s of free precession. The last step was to count the number of neutrons $N_\uparrow$ and $N_\downarrow$ that finished in each of the two polarization states. This was achieved by opening the entrance door to the trap and allowing the neutrons to fall down onto the polarizing foil, which then acted as a spin analyzer. Only those in the initial spin state could pass through to the detector, which was a proportional counter in which neutrons were detected via the reaction $n + {}^3\mathrm{He} \rightarrow {}^3\mathrm{H} + p$. During one-half of the counting period, an rf magnetic field was applied in the region above the polarizing foil; this flipped the spins of the neutrons, thereby also allowing those in the opposite spin state to be counted. Each batch cycle yielded about 14 000 UCN counts. Within a run, the data-taking operations were cycled continuously for 1–2 days. Periodically, after a preset number (normally 16) of batches, the direction of **E** was reversed. All other settings were held constant during a run. Every 10–20 runs, $\mathbf{B}_0$ was reversed so that half of the full data set was taken with $\mathbf{B}_0$ upwards and half with $\mathbf{B}_0$ downwards. We adopt a system as in Ref. [13], where the $\hat{k}$ vector of our z axis follows the direction of $\mathbf{B}_0$. Hence, B_0 is always positive, while the gravitational displacement of the UCNs changes sign.

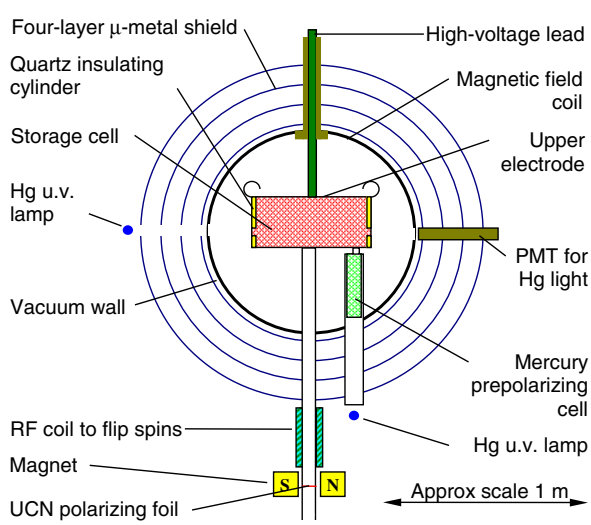

FIG. 1 (color online). Experimental apparatus.

 © 2006 The American Physical Society

The magnetometer used the precession frequency of $I = 1/2$ atoms of ^{199}Hg (3×10^{10} atoms/cm^3; $\mu_n/\mu_{\rm Hg} = \gamma_n/\gamma_{\rm Hg} = -3.842$) stored simultaneously in the same trap as the neutrons. Using Eq. (1) for both UCNs and Hg, and assuming that both experience the same B, we find that to first order in the EDMs d,

$$\frac{\nu_n}{\nu_{\rm Hg}} = \left|\frac{\gamma_n}{\gamma_{\rm Hg}}\right| + \frac{(d_n + |\gamma_n/\gamma_{\rm Hg}| d_{\rm Hg})}{\nu_{\rm Hg}} E = \left|\frac{\gamma_n}{\gamma_{\rm Hg}}\right| + \frac{d_{\rm meas}}{\nu_{\rm Hg}} E. \quad (2)$$

For each run, $d_{\rm meas}$ was obtained from a linear fit to the ratio $\nu_n/\nu_{\rm Hg}$ versus E. Equation (2) shows that $d_{\rm meas}$ contains a contribution from $d_{\rm Hg}$. The true $d_{\rm Hg}$ has been shown to be $(-1.06 \pm 0.49 \pm 0.40) \times 10^{-28} e$ cm [2], so it introduces a bias of $(-0.4 \pm 0.3) \times 10^{-27} e$ cm into $d_{\rm meas}$.

To the true d_n and $d_{\rm Hg}$ within $d_{\rm meas}$, there will also be added coefficients of fractional shifts in ν_n and $\nu_{\rm Hg}$, from other causes, which are linear in E and thus constitute additional systematic errors. The most important of these involves a geometric phase (GP) arising when the trapped particles experience a gradient $\partial B_{0_z}/\partial z$ in the presence of E [13]. Fortunately, the center of gravity of our UCNs is $\Delta h = 0.28$ cm lower than that of the (warmer) Hg atoms, so an observed shift of $\nu_n/\nu_{\rm Hg}$ away from $|\gamma_n/\gamma_{\rm Hg}|$ gives a measure of the volume-averaged $\langle \partial B_{0_z}/\partial z \rangle_V$, via the result [Eq. (86) in Ref. [13]]

$$R_a = \left|\frac{\nu_n}{\nu_{\rm Hg}} \frac{\gamma_{\rm Hg}}{\gamma_n}\right| = 1 \pm \Delta h \frac{\langle \partial B_{0_z}/\partial z \rangle_V}{B_{0_z}}, \quad (3)$$

where the + sign corresponds to $\mathbf{B}_0$ downwards.

In this experiment, the contribution of the GP effect in the Hg to $d_{\rm meas}$ is 50 times larger than the GP effect of the UCNs. Writing the GP false contribution to $d_{\rm meas}$ from the Hg as $d_{n,{\rm Hg},f}$, it is shown in Ref. [13] [Eq. (87)] that

$$d_{n,{\rm Hg},f} = \pm \frac{\hbar}{8} |\gamma_n \gamma_{\rm Hg}| \frac{r_B^2 B_{0_z}}{\Delta h c^2} (R_a - 1) = \pm k (R_a - 1), \quad (4)$$

where r_B is the trap radius and the + sign again corresponds to $\mathbf{B}_0$ downwards. It follows that we can write

$$d_{\rm meas} = d_n' + d_{n,{\rm Hg},f} = d_n' \pm k(R_a - R_{a0}), \quad (5)$$

where d_n' is the true d_n plus all other systematic effects discussed below, and R_{a0} is the value of R_a where $\partial B_z/\partial z = 0$. Equation (5) defines two straight lines, one with positive slope for $\mathbf{B}_0$ down and one with a negative slope for $\mathbf{B}_0$ up. The crossing point (R_{a0}, d_n') provides an estimator of d_n' free of $d_{n,{\rm Hg},f}$.

Each run was made at a chosen value of R_a by preadjusting currents in field-trimming coils. Figure 2 shows the data (binned for clarity) for $d_{\rm meas}$ as a function of R_a for each direction of $\mathbf{B}_0$. The lines represent a least-squares fit to all 554 of the (unbinned) run results, using as free parameters the two intercepts and a common absolute slope k. This yields $\chi^2/\nu = 652/551$ and $k = (1.90 \pm 0.25) \times 10^{-26} e$ cm/ppm, which is within 1.3σ of the expected value of $(1.57 \pm 0.08) \times 10^{-26} e$ cm/ppm from Eq. (4). The slope k can be altered by a few percent (although still remaining highly symmetric under $\mathbf{B}_0$ reversal) by various mechanisms including the UCNs' own GP signal (a 2% effect), uncertainty in Δh (4%), a slight reduction in mean free path due to cavities and grooves in the electrodes as well as to the presence of 10^{-3} torr of He gas to prevent sparks [13,14] (1%), and asymmetric surface relaxation of the Hg (up to 5%).

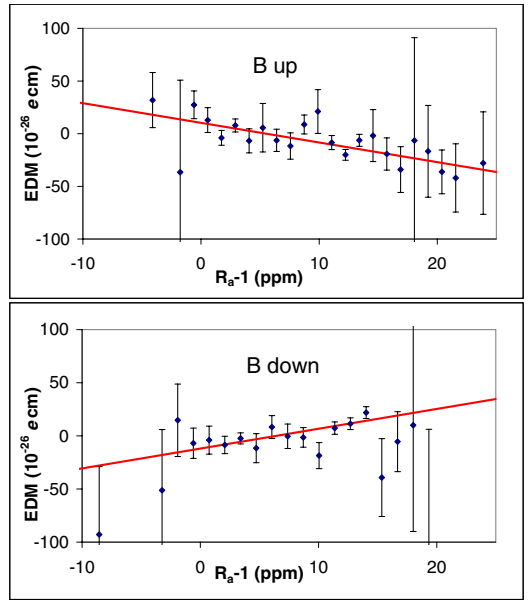

FIG. 2 (color online). Measured EDM (binned data) as a function of the relative frequency shift of neutrons and Hg.

There are some processes that can interfere with the above GP error removal—essentially any process that changes R_a and/or $d_{n,{\rm Hg},f}$ without conforming to the ratio between the two given by Eq. (4) and where, in addition, the changes differ with the direction of $\mathbf{B}_0$.

First, there are several processes that shift R_a but not $d_{n,{\rm Hg},f}$. Changing $\gamma_n/\gamma_{\rm Hg}$ shifts the two lines of Fig. 2 in the same direction by the same amount, leaving d_n' unaffected but changing R_{a0}. We note that our final R_{a0} is consistent with the $\gamma_n/\gamma_{\rm Hg}$ value from the literature ($1\sigma \equiv 1.7$ ppm) [15,16], after allowing for our observed B_x and B_y fields with finite $\partial B_x/\partial y$ and/or $\partial B_y/\partial x$ but with $(\partial B_x/\partial x + \partial B_y/\partial y) = 0 = -\partial B_z/\partial z$ (e.g., a quadrupole aligned with z, with $B_x = qy$, $B_y = qx$), which cause R_a to increase [13] without contributing to $d_{n,{\rm Hg},f}$. Any change in such fields when $\mathbf{B}_0$ is reversed yields a differential shift of all R_a values and thus of the two lines, thereby changing R_{a0} and d_n'. Below, we describe our measurements of the differential shift in R_{a0} and state the correction to d_n'.

B-field averaging in the trap is affected by localized loss of UCN and Hg particles and by polarization loss in the

presence of the 10^{-3} fractional B_0 inhomogeneities, which may change with $\mathbf{B}_0$ direction. However, we estimate that the resulting R_a shifts are <0.1 and <0.01 ppm for the UCN and Hg, respectively, and that they will be indistinguishable from the quadrupole shifts.

Light shifts [17,18] in $\nu_{\rm Hg}$ will shift R_a. They are produced by any small component, parallel to $\mathbf{B}_0$, of the ^{204}Hg probe light beam passing through the precessing ^{199}Hg atoms. This component and the R_a shift reverse sign on reversal of $\mathbf{B}_0$. A slight dependence of R_a on the incident light intensity was indeed found, the magnitude ~0.2 ppm being in agreement with theory. A correction to $d_{\rm meas}$ was made on a run-by-run basis, leading to an overall correction of $(3.5 \pm 0.8) \times 10^{-27} e$ cm.

Second, there are processes that generate an enhanced $d_{n,{\rm Hg},f}$. The field of a permanent magnetic dipole (PMD) close to the trap makes a nonuniform $\partial B_z/\partial z$ and adds an (enhanced) GP $d_{\rm dip}$ [19] to $d_{n,{\rm Hg},f}$ but shifts R_a in accord with Eq. (2) and in opposite senses for the two $\mathbf{B}_0$ directions. The two changes are in a ratio greater than that given by Eq. (4). This shifts the lines of Fig. 2 upwards, adding $(d_{\rm dip} - d_4)$ to d_n', where d_4 is the prediction of Eq. (4) for the $\langle \partial B_z/\partial z\rangle_V$ of this PMD. Our fluxgate-magnetometer surveys of the trap cannot rule out PMD fields of less than 1 nT at 2 cm from the inner surface. Large areas of the trap are SiO_2 or Al, backed by large voids, and do not come under suspicion, but the Hg and UCN doors involve a heterogeneous collection of small parts close to the trap. We allow a d_n' uncertainty of $\pm 6.0 \times 10^{-27} e$ cm to allow for an undetected 1 nT PMD near the Hg door. In the case of the UCN door, we have better diagnostics. The trap used when taking EDM data has a small cavity in the lower electrode, 4.0 cm deep and 6.8 cm in diameter, sealed from below by the door. A PMD in the door mechanism can contribute a $\partial B_z/\partial z$ field to the cavity and to the rest of the trap. The field in the cavity contributes a strong shift in R_a but contributes negligibly via the GP to $d_{n,{\rm Hg},f}$ due to the small cavity radius. The lines of Fig. 2 are thus shifted in opposite directions, again adding to d_n'.

Our additional diagnostics came from separate ν_n, $\nu_{\rm Hg}$, and R_a measurements (without E fields) in two auxiliary traps having roofs that could be raised or lowered to change the height H. The traps were built on the same lower electrode and door mechanism that were used for EDM data taking. Assuming $B_z(z) = b_0 + b_1 z + b_2 z^2$, one can show that $\langle \partial B_z/\partial z\rangle_V = 0$ for a trap height H when $\nu_{\rm Hg}$ is the same for roof settings at $H/2$ and H. With such a field established, R_{a0} was measured for several heights H. The resulting forms of $R_{a0}(H)$ for $\mathbf{B}_0$ up and $\mathbf{B}_0$ down led to the conclusion that there was a dipole field of strength ~1 nT penetrating into the door cavity. They also confirmed the presence of quadrupole fields, which the fluxgate scans showed vary little with H. Polarization data from the EDM runs further substantiated this: UCNs of different energies have different Δhs, so the surviving UCN polarization decreases in proportion to $(\partial B_z \partial z)^2$, and the values of R_{a0} where the $\mathbf{B}_0$ up and down polarizations peak are in excellent agreement with the auxiliary trap results.

The first auxiliary trap used had a smaller radius, 18.5 rather than 23.5 cm, and a cavity depth of 6.0 rather than 4.0 cm. These differences amplify the R_a shifts from a dipole field in the cavity by 1.50 and reduce the quadrupole shifts by a factor 1/1.8. Our systematic-error correction to d_n' to allow for the combined door dipole and quadrupole fields is $(0.69 \pm 0.28) \times 10^{-26} e$ cm. The auxiliary trap used to measure Δh by obtaining R_a as a (linear) function of a series of known $\langle \partial B_z/\partial z\rangle_V$ was made as similar to the data-taking trap as possible in dimensions and materials so as to reproduce the same UCN velocity spectrum.

We now consider the systematic errors not involving GP, beginning with the first-order $\mathbf{v} \times \mathbf{E}$ effects.

If the UCNs have a net translational motion, any perpendicular component of $\mathbf{E}$ will be seen in their rest frame as a combination of $\mathbf{E}$ and $\mathbf{B}$ fields. During the Ramsey measurement period, the UCN ensemble may warm slightly due to vibrations, causing the center of mass to rise by up to 0.1 cm. If the volume-averaged angles between $\mathbf{E}$, $\mathbf{B}$, and $\mathbf{v}$ are each as high as 0.05 radians, the induced false EDM will be $0.03 \times 10^{-27} e$ cm.

Similarly, any net rotational flow of the UCN in conjunction with a radial $\mathbf{E}$ component may lead to an induced EDM signal. However, any such flow of UCN will be attenuated by wall collisions before the first Ramsey pulse is applied. We calculate that the maximum error to be expected from this source and from higher-order $\mathbf{v} \times \mathbf{E}$ effects is below $1 \times 10^{-27} e$ cm.

Analysis of the data suggested a small correlation between the intensity of the Hg reading light and the value of the applied $\mathbf{E}$ field. Through the light shift, this could directly create an EDM signal. However, to within its uncertainty, the dependence of R_a on the light intensity has been removed. The residual systematic uncertainty from this source is $0.2 \times 10^{-27} e$ cm.

There may also be residual effects from $\mathbf{B}$-field fluctuations. For example, a dipolelike field $\mathbf{B}_d$ originating from the μ-metal in the region of the HV feedthrough would be sensed by both neutrons and Hg but with a difference given by $\delta B_d/B_d = 3\Delta h/r$, where $r \sim 55$ cm is the distance from the source of the field to the center of the bottle. Thus, fluctuations in $\mathbf{B}$ that are correlated with the HV can be expected to be compensated up to a factor of about 70. In order to study this, the Hg and neutron channels were analyzed independently. The neutrons yielded an EDM signal of $(17 \pm 4) \times 10^{-26} e$ cm; the Hg, once the GP contribution (as calculated from the average $R_a - 1$ at which the data were taken) was subtracted, yielded $(-3.9 \pm 0.8) \times 10^{-26} e$ cm. These results are consistent with a common source of magnetic fluctuations correlated with the HV. We therefore expect the Hg compensation to shield us from this systematic effect to a level of $17 \times 10^{-26}/70 = 2.4 \times 10^{-27} e$ cm.

Electrostatic forces may move the electrodes slightly. In conjunction with a finite $\partial B/\partial z$, an HV-dependent shift in

TABLE I. Systematic errors and uncertainties ($10^{-27}e$ cm).

Effect	Shift	σ
Door cavity dipole	−5.6	2.0
Other dipole fields	0.0	6.0
Quadrupole difference	−1.3	2.0
$\mathbf{v} \times \mathbf{E}$ translational	0.0	0.03
$\mathbf{v} \times \mathbf{E}$ rotational	0.0	1.0
Second-order $\mathbf{v} \times \mathbf{E}$	0.0	0.02
ν_{Hg} light shift (geo phase)	3.5	0.8
ν_{Hg} light shift (direct)	0.0	0.2
Uncompensated B drift	0.0	2.4
Hg atom EDM	−0.4	0.3
Electric forces	0.0	0.4
Leakage currents	0.0	0.1
ac fields	0.0	0.01
Total	−3.8	7.2

the ratio would then appear, showing up as an EDM-like signal but with $\Delta\nu$ proportional to $|\mathbf{E}|$ instead of to $\mathbf{E}$. Different HV magnitudes for the two signs of $\mathbf{E}$ could then generate a false EDM signal. The $|\mathbf{E}|$ signal was found to be $-1.5 \pm 3.8 \times 10^{-26}e$ cm. The measured HV and charging currents show that the HV magnitude was the same for both polarities to within <1%. This systematic uncertainty is therefore $0.4 \times 10^{-27}e$ cm.

Analysis of the EDM as a function of leakage current shows no measurable effect. Leakage currents are typically of order 1 nA. If this current were to travel 10 cm azimuthally around the bottle, the resultant $\mathbf{B}$ field would result in an apparent EDM of $0.1 \times 10^{-27}e$ cm.

ac fields were also studied. There is no differential ripple visible on the HV at the level of a few volts. Sampling is done at 5 Hz with a bandwidth of 20 kHz, so any 50 Hz ripple would show up as beats. This is certainly absent at the level of 50 V, which would give a false EDM of $0.01 \times 10^{-27}e$ cm. Low-frequency ac fields were sought by means of a pickup coil in conjunction with a phase-sensitive detector. Shifts in R_a from this source at the level of 0.02 ppm could not be ruled out. Cancellations in the corresponding EDM signal from reversals of the electric and magnetic fields would reduce any net contribution to below the level of $0.01 \times 10^{-27}e$ cm.

Two approaches were adopted in studying the data. In the first analysis, only the 293 runs with an uncertainty on R_a of less than 0.05 and with $-10\ \mathrm{ppm} < (R_a - 1) < 21\ \mathrm{ppm}$ were accepted. As the two resulting average $R_a - 1$ values (8.948 and 8.943 ppm for $\mathbf{B}_0$ up and down, respectively) were almost identical, with approximately equal amounts of data in each field direction, a weighted average of the d_{meas} data was used as an estimator of d_n. The result was

$$d_n = (-0.2 \pm 1.6(\mathrm{stat})) \times 10^{-26}e\ \mathrm{cm}(\chi^2/\nu = 1.24),$$

with an additional uniformly distributed systematic uncertainty of $\pm 1.2 \times 10^{-26}e$ cm allocated to it in order to accommodate any potential systematic biases arising from the effects listed in Table I. The resulting distribution implies $|d_n| < 2.9 \times 10^{-26}e$ cm (90% C.L.).

The second analysis began with the Fig. 2 fitted-lines crossing-point value $d_n' = (-0.55 \pm 1.51) \times 10^{-26}e$ cm (which includes the run-by-run light shift correction) and then applied the systematic-error corrections given in Table I. The final result from this approach is

$$d_n = (+0.2 \pm 1.5(\mathrm{stat}) \pm 0.7(\mathrm{syst})) \times 10^{-26}e\ \mathrm{cm},$$

implying $|d_n| < 2.8 \times 10^{-26}e$ cm (90% C.L.).

The data set analyzed here, which excludes data that have already been published [1], incorporates all measurements undertaken between the autumn of 1998 and the end of 2002. The results overall may be interpreted as an upper limit of $|d_n| < 2.9 \times 10^{-26}e$ cm (90% C.L.).

The authors are grateful to N. F. Ramsey for many useful discussions, to Y. Chibane, M. Chouder, and I. A. Kilvington for contributions during development, to E. N. Fortson's group for information and components relating to Hg magnetometry, to R. Baskin for simulation work, and to the ILL for its provision of neutron facilities. The work was funded by grants from the UK's PPARC. Support from the RFFI, via Grant No. 03-02-17305, is gratefully acknowledged by S. N. I.

*On leave from Institute of Nuclear Research and Nuclear Energy, Sofia, Bulgaria.
†On leave from PNPI, Russia.

[1] P. Harris *et al.*, Phys. Rev. Lett. **82**, 904 (1999).
[2] M. Romalis *et al.*, Phys. Rev. Lett. **86**, 2505 (2001).
[3] B. Regan *et al.*, Phys. Rev. Lett. **88**, 071805 (2002).
[4] R. Peccei and H. Quinn, Phys. Rev. Lett. **38**, 1440 (1977).
[5] X.-G. He *et al.*, Phys. Rev. Lett. **61**, 1267 (1988).
[6] S. Barr, Int. J. Mod. Phys. A **8**, 209 (1993).
[7] N. Ramsey, in *Proceedings of the XIV International Conference on Atomic Physics* (AIP, New York, 1994), p. 3.
[8] J. Ellis and R. Flores, Phys. Lett. B **377**, 83 (1996).
[9] O. Lebedev *et al.*, Phys. Rev. D **70**, 016003 (2004).
[10] M. Pospelov and A. Ritz, Ann. Phys. (N.Y.) **318**, 119 (2005).
[11] S. Abel and O. Lebedev, J. High Energy Phys. 01 (2006) 133.
[12] K. Green *et al.*, Nucl. Instrum. Methods Phys. Res., Sect. A **404**, 381 (1998).
[13] J. Pendlebury *et al.*, Phys. Rev. A **70**, 032102 (2004).
[14] S. Lamoreaux and R. Golub, Phys. Rev. A **71**, 032104 (2005).
[15] G. Greene *et al.*, Phys. Rev. D **20**, 2139 (1979).
[16] B. Cagnac, Ann. Phys. (Paris) **6**, 467 (1961).
[17] C. Cohen-Tannoudji and J. Dupont-Roc, Phys. Rev. A **5**, 968 (1972).
[18] A. Corney, *Atomic and Laser Spectroscopy* (Oxford University, New York, 1968).
[19] P. Harris and J. Pendlebury, Phys. Rev. A **73**, 014101 (2006).